

# Optical Magnetometry Using Nitrogen-Vacancy Centers

MICHAEL ONYSZCZAK

*Department of Physics and Astronomy, Iowa State University, Ames, IA 50011, U.S.A.*

Submitted: August 18, 2017

Revised: October 19, 2017

---

**The search for highly sensitive magnetometers has been a particularly active area of condensed matter research, especially for nuclear magnetic resonance (NMR) applications. Negatively Charged Nitrogen-Vacancy ( $NV^-$ ) sites in diamond provide a sensitive solid-state magnetometer which can detect magnetic fields with sensitivities on the order of  $pT/\sqrt{Hz}$ . We demonstrate the practical ability to use this system to measure the bulk magnetization of a variety of magnetic materials at ambient temperature and pressure as the first step to incorporating this system into a low-temperature, high-pressure magnetic measurement system.**

---

## INTRODUCTION

Magnetometers have found extensive use in both traditional physics research (such as nuclear magnetic resonance (NMR) studies and bulk material characterization) and in more applied fields such as medicine and archaeology [1][2]. The research and development of high sensitivity (order  $nT/\sqrt{Hz}$ ) magnetometers have been particularly active, but one current limitation of existing magnetometers is their large detector-sample separation distance [3]. Since magnetic fields decay as  $r^{-3}$ , minimizing sensor size and sample-detector separation is essential for high sensitivity nanoscale characterization of materials.

Recently, the use of nitrogen-vacancy (NV) centers within diamond have been proposed for use as a solid-state magnetometer. This system provides a nanoscale, solid-state magnetometer which can achieve sensitivities on the order of  $pT/\sqrt{Hz}$  [4]. Currently, these magnetometers have been used for magnetic imaging, and have been able to detect a single proton spin and spatially locate it to within 1 nm [5]. This type of magnetometer would also be particularly useful in conducting NMR experiments as the sensitivity needed to detect a small number of nuclear spins remains one of the limiting factors in NMR research. Similarly, this type of magnetometry would be useful in a number of high-pressure measurement devices where there is a limited amount of physical space to place a detector.

## NITROGEN VACANCY CENTERS

Nitrogen-vacancy sites are one of many types of defects in type I-b diamond. Type I-b diamonds are grown in high nitrogen environments and then irradiated with

high energy ( $\sim 1$  MeV) electrons to create vacancies within the carbon lattice. The NV's form where one carbon atom is substituted by a nitrogen atom and there is a vacancy in an adjacent carbon site. The NV lies along one of the four body-diagonal (111) crystallographic axes and possesses the three-fold rotation  $C_{3V}$  symmetry [6][7]. The NV center can gain an additional electron from a nitrogen impurity elsewhere in the lattice, and this causes the NV center to gain a net negative charge (referred to as  $NV^-$ ) [8]. Uncharged NV sites also exist within the diamond, but their electronic properties are less interesting for use in magnetometry and will not be discussed further.

The electronic structure of the  $NV^-$  system is shown in figure 1. Six electrons are associated with the  $NV^-$  system. The six electrons come from the following sources: three electrons from the three carbons nearest to the vacancy (which normally form bonds with the carbon atom that sits in the vacancy site), two electrons from the nitrogen impurity (the other three nitrogen valence electrons are bonded with its surrounding carbon atoms), and the one electron from a non-local substitution nitrogen atom. However, it is oftentimes easier to simply see this system as a two-hole spin 1 system instead of a more complex six electron system, but either view will result in identical electronic structures [9].

This spin 1 system possesses  $C_{3V}$  symmetry, and the resulting electronic structure of such a system is well known and has the following states. The ground state is a triplet with state symmetry  $^3A_2$ , and in zero-field the  $^3A_2$  states,  $m_s = |0\rangle$  and  $m_s = |\pm 1\rangle$ , are separated by an energy gap of  $D_{gs} = 2.87$  GHz which arises primarily due to spin-lattice interactions. The excited triplet state has  $^3E$  symmetry, and its  $m_s = |0\rangle$  and  $m_s = |\pm 1\rangle$  states are separated by an energy

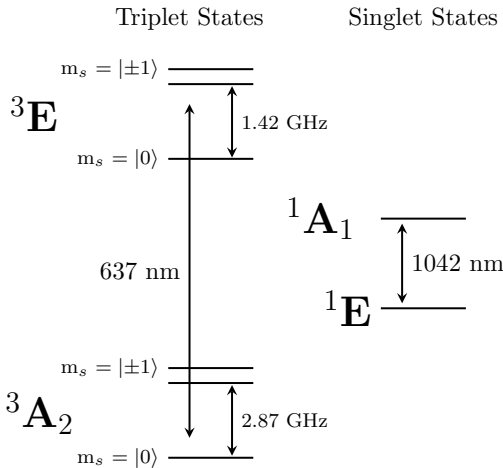


**FIGURE 1.** Electronic Structure of an  $NV^-$  system with triplet states on the left and singlet states on the right. The mixed-use of wavelength and frequency is due to experimental conventions where the ground to excited state transitions are associated with optically driven transitions where wavelength is typically used and the transitions between  $m_s$  states are driven by microwaves where frequency is typically used.

$D_{gs} = 1.42 \text{ GHz}$ [10]. If a non-zero magnetic field is applied then the  $m_s = |\pm 1\rangle$  will lose their degeneracy via the Zeeman effect and gain an energy splitting given by  $\Delta E = \gamma \hbar H$  where  $H$  is the applied magnetic field and  $\gamma = 2\pi \times 28 \text{ GHz/T}$

This system allows for transitions from states with the same value of  $m_s$ , and there is a triplet-singlet transition from the  ${}^3E$ ,  $m_s = |\pm 1\rangle$  state to the  ${}^1E$  state and from  ${}^1A_1$  to  ${}^3A_2$   $m_s = |0\rangle$  [11]. This particular relaxation pathway has a lifetime of  $\leq 1 \text{ ns}$  and is non-fluorescing. This non-fluorescing relaxation pathway (seen in figure 2) is only available to due to spin-spin interaction and only is present for the excited  $m_s = |\pm 1\rangle$  states[12].

The heart of  $NV^-$  magnetometry relies on a double excitation process first using microwave radiation tuned to energy gap of the  $|0\rangle \rightarrow |\pm 1\rangle$  transition. The second excitation uses a laser to transition from the ground state to the excited state. From the excited state, the system will relax partially through emitting radiation and directly transitioning from the excited state to the ground state and partially through non-radiative relaxation through the singlet states. However, if the microwave radiation is not matched to the energy gap between the  $|0\rangle$  and  $|\pm 1\rangle$  states then the system will only relax via fluorescence since the transition to the singlet state is only possible from the  $|\pm 1\rangle$  excited state and laser-driven excitation alone cannot cause transitions from the  $|0\rangle$  to the  $|\pm 1\rangle$  states. The drop in fluorescence associated with providing the microwave

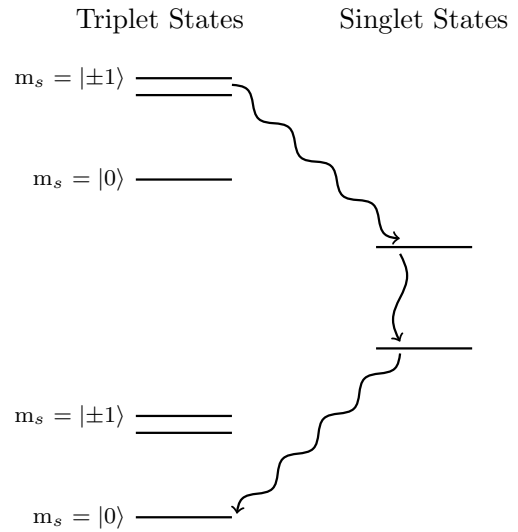


**FIGURE 2.** The non-fluorescing relaxation pathway from the excited  $m_s = |\pm 1\rangle$  state.

frequency needed to excite the  $|0\rangle \rightarrow |\pm 1\rangle$  transition reveals the field that the  $NV^-$  centers are experiencing.

## EXPERIMENTAL METHODS

$NV^-$  magnetometry was performed by using a 532 nm, 5 mW laser to provide the energy for the transition between the ground and excited states. 532 nm is chosen as a red light filter can be used on the photo-diode to remove any reflected laser radiation to ensure that only fluorescence is being measured. Additionally, using a higher energy excitation energy only results in phonon production which does not affect the experiment. An *HP 5565A* frequency generator to produce microwaves to excite the  $|0\rangle \rightarrow |\pm 1\rangle$  transition. The optical diagram below (figure 3) shows the general set-up used to focus the laser onto the diamond containing the  $NV^-$ 's and the process used to collect and detect the fluorescence from the diamond using an Avalanche Photo-diode (APD) which generates a voltage that is proportional to the intensity of the incoming light.

In order to better isolate the signal of the fluorescence from noise and ambient light, the microwave power underwent amplitude modulation at 1 kHz, and a *SR510* lock-in amplifier matched to the modulation frequency was used to isolate the now oscillating fluorescence signal. The lock-in amplifier allowed for shorter averaging times to be used and improved the overall signal to noise ratio.

In order to deliver the microwave radiation two different systems were used. The first method used a microwave strip line on a printed circuit board with a 1.5 mm loop to deliver the microwave radiation to the  $NV^-$  containing diamond (figure 4). This system allowed for a larger  $NV^-$  containing diamond to be used, which

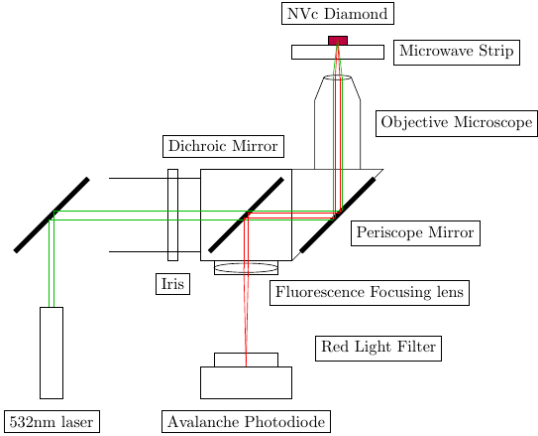


**FIGURE 3.** The optical set-up used to deliver light to and from the  $NV^-$  diamond

increased overall fluorescence as a larger number of  $NV^-$  sites were illuminated and allowed large bulk samples to be placed on top of the  $NV^-$  containing diamond for characterization. The main disadvantage of this system was that it was forced to be at ambient conditions which limit the type of characterization that could be done.

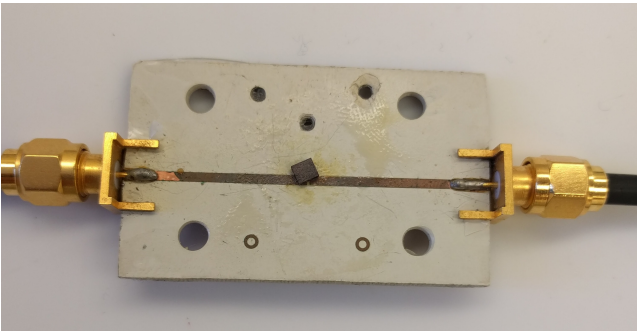


**FIGURE 4.** The microwave strip board showing a  $25 \text{ mm}^2$  NV diamond for scale.

The second set-up used to deliver microwaves was a custom diamond anvil cell. This diamond anvil cell has one of its pressure delivering diamonds embedded with a thin tungsten coil with external leads that embedded through the side of the diamond (figure 5). This coil could be connected externally to the microwave power source to deliver microwaves directly into the sample cavity of the diamond anvil cell. The  $NV^-$  containing diamonds used in this set-up were single crystalline micro-diamonds  $< 15 \mu\text{m}$  in size.

In order to perform magnetometry, various samples (elemental cobalt, elemental gadolinium, and single crystalline MnBi) were placed on top of the  $NV^-$  diamond, a magnetic field was applied, a spectrum was taken, and then the sample was removed to repeat this process with only the  $NV^-$  containing diamond. This yields two curves (figure 6) which show how the splitting

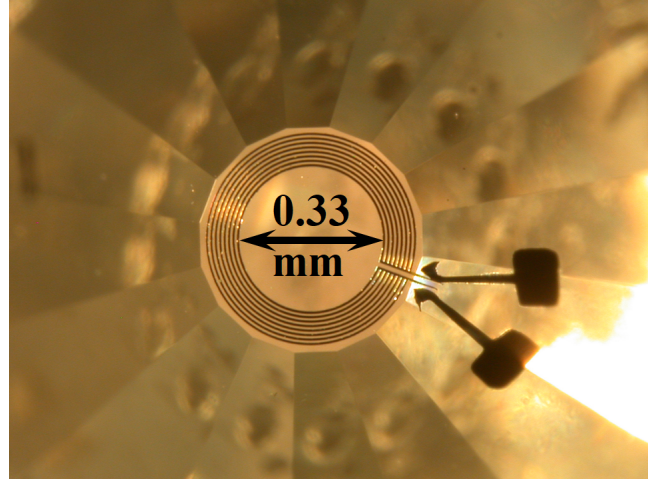


**FIGURE 5.** Diamond with microwave coil embedded in surface with inner diameter for scale

between the  $|\pm 1\rangle$  spin states is affected by an applied magnetic field. The difference in splitting between having a sample and not having a sample on top of the  $NV^-$ 's gives a measure of the magnetic response of the sample to the external magnetic field.

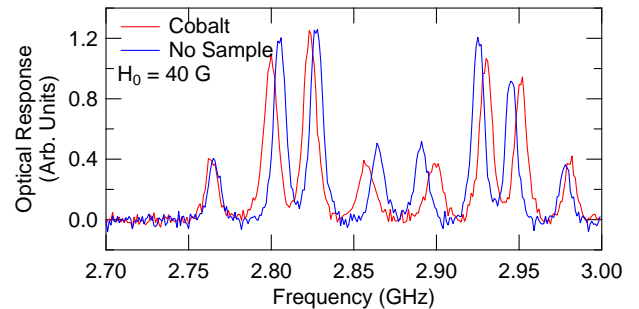


**FIGURE 6.** Difference in spectral splitting between the  $NV^-$  sites with a cobalt sample and  $NV^-$  sites alone. The eight peaks represent the the energy level of the  $|0\rangle \rightarrow |\pm 1\rangle$  states of each of the four crystallographic orientations of the  $NV^-$  sites

The pressure dependence of the  $NV^-$  spectrum was also examined by using a single  $NV^-$  containing microdiamond in the diamond anvil cell with several pieces of ruby. The diamond anvil cell was pressurized using Daphne Oil 7373 as the pressure medium. The ruby pieces were used to conduct ruby fluorescence to determine the pressure present within the diamond anvil cell. The cell was then aligned in the optical set-up and zero-field scans of microwave frequencies were performed to study the behavior of the  $NV^-$  spectrum under pressure.

## RESULTS

Three different magnetic samples were characterized using this system: elemental cobalt, elemental

gadolinium, and single crystalline MnBi and their dipolar magnetic response are seen in figure 7. The dipolar field, which is proportional to the internal magnetization of the sample via equation 1 (where  $\chi$  is the magnetic susceptibility,  $H$  is the applied field,  $V$  is the volume of the sample,  $M$  is the bulk magnetization of the sample, and  $r$  is the separation between the sample and the  $NV^-$  centers).

$$H_{dipole} \sim \frac{\chi HV}{r^3} = \frac{MV}{r^3} \quad (1)$$

In the case of elemental cobalt which is a hard ferromagnet and remains magnetic up to 1400 K, we would expect a non-zero remanence which implies that there is some finite magnetization at zero applied field, and we would expect to see a linear magnetization trend at such low fields since the sample is not close to saturation yet. This is clearly seen by the large intercept and the comparatively large slope observed in figure 7.

Elemental gadolinium at room temperatures is just above its Curie temperature of 293K, so its expected paramagnetic behavior would have zero magnetization at zero applied field and a small (compared to the ferromagnetic samples) magnetic susceptibility as observed in figure 7.

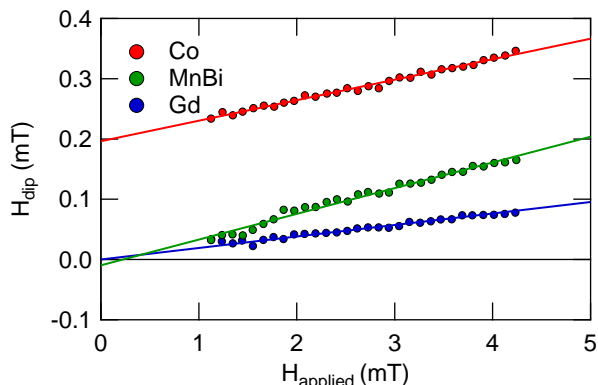


**FIGURE 7.** Magnetic response of various materials

A single crystal of MnBi would have a large susceptibility, as it is ferromagnetic, and zero or almost zero magnetization at zero applied field since a single crystal has no pinning mechanisms to develop remanent magnetization, and the only field that could be sensed at zero applied field would be a surface domain which would have an extremely small remanence compared to the remanence of a hard ferromagnetic material like cobalt.

The results of the pressure dependence of the NV spectrum can be seen in figure 8. The most striking feature of these spectra is that the zero field energy gap between the ground state  $|0\rangle$  and  $|\pm 1\rangle$  states has a linear dependence on pressure, shown in figure 9. The linear relationship determined here (11.73(3)

MHz/GPa) is smaller than the previously published value of 14.58(6) MHz/GPa [13]. This is likely due to our pressure medium reaching its hydrostatic limit and solidifying, which Daphne Oil 7373 does at 2.3 GPa [14]. Uniaxial strain on the  $NV^-$  centers is believed to cause deformations to the diamond lattice which directly impact the  $NV^-$  spectrum and its zero-field behavior.

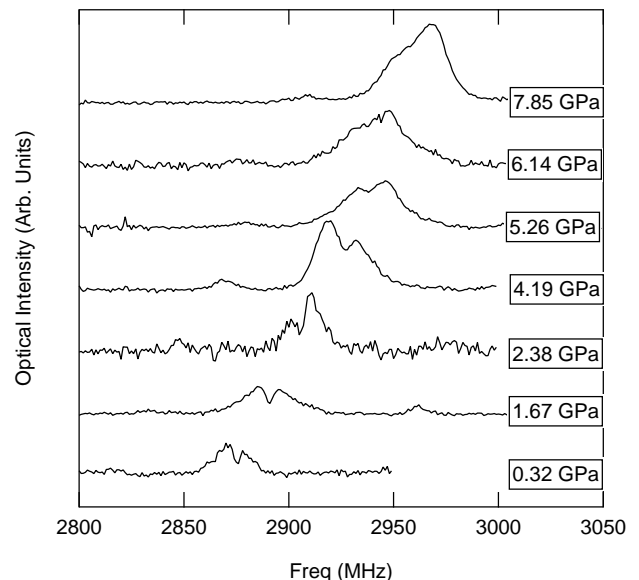


**FIGURE 8.** Pressure Dependence of the  $NV^-$  Spectrum

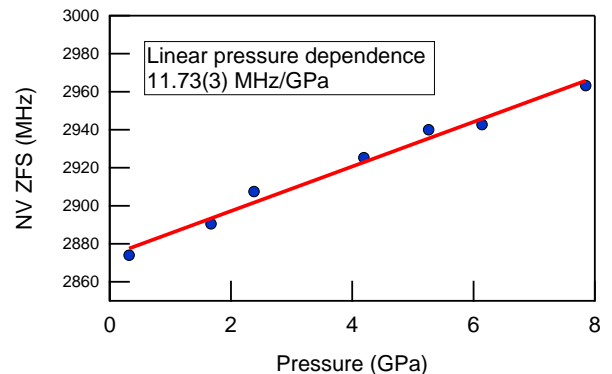


**FIGURE 9.** Relationship between Zero-Field Ground State Splitting and Pressure

## DISCUSSION & FUTURE WORK

The magnetometry performed on elemental cobalt, elemental gadolinium, and single crystalline MnBi confirms that this magnetometer has the capability to characterize magnetic materials under ambient conditions using the microwave strip board.

The next major step for developing this magnetometer is to replicate the measurements performed on

the microwave board in the diamond anvil cell at ambient pressures. A major difficulty is that the diamond anvil cell is space limited so the size of the material to be studied must be reduced which in turn reduces its magnetic dipole signal. Additionally, aligning to a single NV<sup>-</sup> microdiamond on the size  $\sim \mu\text{m}^3$  will have a much smaller fluorescence than the 25 mm<sup>3</sup> diamond used on the microwave strip board which will cause this measurement to have a much lower signal to noise ratio. Also to ensure only hydrostatic pressure is applied to the NV<sup>-</sup> containing diamond, a new pressure medium must be found that can resist the high pressures within the diamond anvil cell.

The second step would be to incorporate a fiber optic system into the set-up to deliver the laser light and collect the fluorescence remotely. This would allow the diamond anvil cell to be easily moved into a cryostat which allows for temperature control and the use of superconducting magnets to apply large external fields.

The final goal of this project is to use this probe not only to characterize the bulk magnetization of samples in DC magnetic fields, but to eventually perform NMR type sequences to study not only the electron response of NV<sup>-</sup>'s to microwave radiation, but also how the electrons in this system couple to the nuclear moments of a sample. This type of system could easily be used to probe both local and non-local electron interactions and provide a more precise measurement tool to characterize various materials.

## ACKNOWLEDGEMENTS

I would like to thank Dr. Nick Curro and Louis Steele for their advice and their help with this

project. Additional thanks to Dr. Valentin Taufour for producing samples used in our magnetization measurements and to the Pines group at UC Berkeley for allowing us to use portions of their NV<sup>-</sup> optical set-up. Finally, I would like to thank the National Science Foundation for funding this REU, and I would like to thank Rena Zieve for her support and organization of this program.

## REFERENCES

- [1] C. Gaffney, *Archaeometry* **50**, 313 (2008).
- [2] R. Hari and R. Salmelin, *NeuroImage* **61**, 386 (2012).
- [3] P. Ripka and M. Janosek, *IEEE Sensors Journal* **10**, 1108 (2010).
- [4] T. Wolf et al., *Phys. Rev. X* **5**, 041001 (2015).
- [5] M. Loretz et al., *Science* (2015).
- [6] G. Davies and M. F. Hamer, *Proc. R. Soc. London Ser. A* **348**, 285 (1976).
- [7] A. Gali, *Phys. Rev. B* **80**, 241204 (2009).
- [8] J. H. N. Loubser and J. A. van Wyk, *Rep. Prog. Phys.* **41**, 1201 (1978).
- [9] L. M. Pham, *Magnetic Field Sensing with Nitrogen-Vacancy Color Centers in Diamond*, PhD thesis, Harvard University, 2013.
- [10] M. W. Doherty et al., *Physics Reports* **528**, 1 (2013), The nitrogen-vacancy colour centre in diamond.
- [11] V. M. Acosta, A. Jarmola, E. Bauch, and D. Budker, *Phys. Rev. B* **82**, 201202 (2010).
- [12] L. J. Rogers, S. Armstrong, M. J. Sellars, and N. B. Manson, *New Journal of Physics* **10**, 103024 (2008).
- [13] M. W. Doherty et al., *Phys. Rev. Lett.* **112**, 047601 (2014).
- [14] K. Yokogawa, K. Murata, H. Yoshino, and S. Aoyama, *Japanese Journal of Applied Physics* **46**, 3636 (2007).